Appl. Phys. A 70, 93–96 (2000) / Digital Object Identifier (DOI) 10.1007/s003399900147

Applied Physics A
Materials
Science & Processing

Study of photoluminescence and electronic states in nanophase strontium titanate

W.F. Zhang, Z. Yin, M.S. Zhang*

National Laboratory of Solid State Microstructures and Center for Materials Analysis, Nanjing University, Nanjing 210093, P.R. China

Received: 9 March 1999/Accepted: 29 July 1999/Published online: 3 November 1999

Abstract. Nanophase strontium titanate specimens were prepared by a stearic acid sol-gel process. The phase structures, photoluminescence, and electron states were investigated by X-ray diffraction and fluorescence spectroscopy. A visible emission band centered at 500 nm was observed in the nanosized particles under an excitation with energy lower than the band gap at room temperature. The peak intensity of the visible emission band increases with decreasing particle size. This visible emission is attributed to the recombination of the long-lived self-trapped excitons with forceful binding-energy formed in the nanosized $SrTiO_3$ mediated by the localized levels which are correlated to the intrinsic surface states and defect centers via a strong electron–phonon interaction. The dependence of the visible emission band on excitation wavelength was examined under both room and liquid nitrogen temperatures where there exist a series of levels of the self-trapped excitons within the forbidden gap and the properties of the self-trapped states are closely related to temperature.

PACS: 79.60.-i; 73.20.At; 81.40

Photoluminescence (PL) properties of the nanosized materials have attracted considerable attention in the past decades [1–3]. It is quite natural that the nanosized materials show different optical properties from those of bulk materials. On the one hand, the approaching of the particle diameter to the order of some characteristic parameters, such as the de Broglie wavelength of conductive electron, Bohr radius of exciton, and correlation length, etc. can cause a quantum confinement effect, such as in the nanostructured Si, Ge semiconducting systems, and on the other hand, the peculiar structure of the nanosized materials, i.e., a large number of intrinsic surface states and defect centers exert an important influence on their electronic state properties.

$SrTiO_3$ is a well-known perovskite-type incipient ferroelectric with a large dielectric constant. In addition to its acoustic, dielectric, and piezoelectric properties studied extensively [4–6], its electronic structure and optical properties have also been investigated theoretically and experimentally. The calculation by Kahn and Leyendecher using the linear combination of atomic orbitals (LCAO) method showed that the fundamental band gap is indirect, and the filled valence bands are derived from oxygen $2p$ orbitals and the empty conduction bands derived from titanium $3d$ orbitals [7]. The band gap deduced from the observed optical absorption edge ranges from 3.2 to 3.4 eV [8, 9]. This uncertainty is mainly due to occurrence of the extended Urbach tail, which is often found in $BaTiO_3$, $PbTiO_3$, TiO_2, and the other related compounds containing TiO_6 octahedra [10]. It is apparent that bulk $SrTiO_3$ absorbs ultraviolet (UV) radiation, and the optical absorption corresponds to a charge-transfer transition between O^{2-} and Ti^{4+} localized within a regular octahedron. Grabner [11] and Sihvonen [12] reported photoluminescence of single-crystal $SrTiO_3$, a broad and structureless visible emission band peaked around 500 nm under UV radiation at low temperature. Investigation on temperature dependence of the visible emission demonstrated that the visible emission band was quenched at temperatures above 110 K. Many experiments, such as radio luminescence [13], cathodoluminescence [10], and X-ray induced luminescence [14], etc. have been performed and not given uniform explanations for the mechanism of the visible emission. Using time-resolved spectroscopy, Leonelli and Brebner proposed a model to describe the luminescence process where electrons form small polarons and holes interact with the polarons to produce self-trapped excitons (STEs), and the recombination of STEs results in the visible emission, either immediately, or after being trapped for a certain time by impurities and defects [15, 16]. However, disappearance of the visible emission above 110 K has not been well explained yet.

Recently, more attractive optical and PL properties have been revealed in bulk $SrTiO_3$, for example, three-photon transitions, self-oscillations of excitons, and ionization of excitons by laser radiation [17–19]. In particular, room-temperature PL caused by the particle size effect in nanophase $ATiO_3$ (A = Sr, Ba, Pb, and $La_{0.5}Na_{0.5}$) has also been reported [20–22]. These arouse a renewed interest in studying

* Corresponding author.
(Fax: +86-25/3595535, E-mail: mszhang@netra.nju.edu.cn)

the PL and electronic states of the nanophase $SrTiO_3$. In this paper we have synthesized the nanophase $SrTiO_3$ samples, and investigated their photoluminescence properties at different particle sizes, excitation wavelengths as well as temperatures to gain a better understanding of the PL processes.

1 Experimental

Nanophase $SrTiO_3$ samples were synthesized using a stearic acid sol-gel method with starting precursors of strontium stearate and tetrabutyl titanate and solvent of the melted stearic acid (70 °C). After gelation the samples were heat-treated for 3 h at different temperatures: 650, 750, 850, and 900 °C. X-ray diffraction patterns show their cubic structure with well-crystallized character of the nanophase specimens. Their average grain sizes were obtained from the XRD patterns via Scherrer's equation [23], $D = k\lambda/\beta(\theta)\cos\theta$, where D is the average grain diameter, k the constant (shape factor about 0.9), λ the X-ray wavelength, $\beta(\theta)$ the full width at half maximum (FWHM) of the given diffraction line (here the (111) line is used), and θ the diffraction angle. The corresponding mean sizes of the nanocrystals are as follows: 26, 50, 120, and 286 nm. In order to facilitate PL measurements, the $SrTiO_3$ powders were compressed into discs with diameter of 13 mm and thickness of 2 mm.

X-ray diffraction measurements were conducted by X-ray diffractometer with model D/Max-RA and the PL measurements were carried out on a SPEX F212 Fluorescence spectrometer where a xenon lamp with 150 mW power output was used as an excitation source.

2 Results and discussion

Figure 1 shows the PL emission spectra of the nanophase $SrTiO_3$ specimens under an excitation of 398 nm at room temperature. It can be seen that the nanophase $SrTiO_3$ with particle size of 286 nm has almost no luminescence, similar to the case of the bulk material. However, a broad visible emission band appears around 500 nm when the particle size decreases to 120 nm. Also, the peak intensity of the visible emission band increases rapidly with decrease of the particle size, while the corresponding peak position shows no shift.

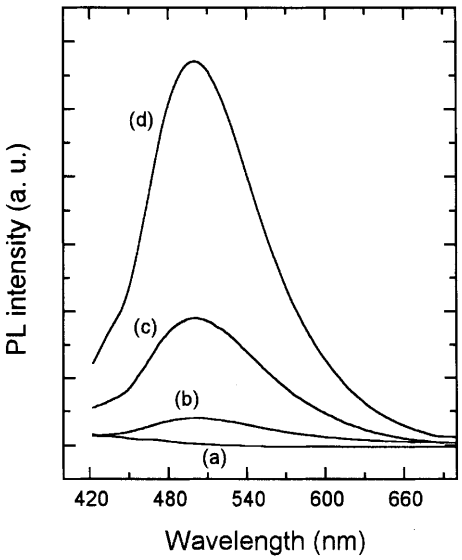

Fig. 1. PL spectra of the nanophase $SrTiO_3$ under excitation at 398 nm for various particle sizes: (a) 286 nm, (b) 120 nm, (c) 50 nm, and (d) 26 nm

It is noted that both the excitation energy of 3.1 eV (398 nm) and the observed emission maximum energy (2.6 eV) lie within the band gap of $SrTiO_3$, which shows that there must exist certain localized levels within the forbidden gap because the direct electron transition between the valence band and the conduction band should be not allowed. However, a large number of surface "broken" or dangling bonds and defect centers intrinsically existing in the nanosized materials, can form various animated energy levels localized within the forbidden gap and act as the optical absorption centers, which make large modification for the optical properties of materials such as CdS [1] and TiO_2 [2]. For the nanosized titanates, the remarkable effects of the surface states and defect centers on their optical and photoelectric properties were also found in the study of surface photovoltaic of the nanophase $PbTiO_3$ [24] and photoacoustic spectroscopy of the nanophase $SrTiO_3$, $NiTiO_3$, and $CoTiO_3$ [25, 26]. Owing to their structural characters the (001) plane including O^{2-} and Ti^{4+} in $ATiO_3$ (A = Sr, Ba, Pb) is very easily exposed at interfaces [27, 28] and therefore would produce a large number of the "broken" bonds of Ti and O atoms in such nanosized materials. It has been experimentally elucidated that the d-orbital surface states formed by Ti^{3+} are stabilized in the forbidden gap at a certain concentration of oxygen deficiencies [29]. It is obvious that the number of the intrinsic surface states and defect centers, and thus the intensity of the visible emission band will increase with decrease of the particle size.

There is a strong electron–phonon interaction in the bulk $SrTiO_3$. This becomes much stronger in the nanophase system than in the bulk phase due to the remarkable dielectric and phonon confinement effects [30, 31], thus the formation of the STE in the nanophase $SrTiO_3$ is certainly unavoidable. It is known that the binding energy and the radiative lifetime of the excitons are strongly related to the particle size [3]. It is believed that the long-lived STE with forceful binding energy can be formed, resulting in the visible emission in the nanophase $SrTiO_3$ even at room temperature. A possible PL process is shown in Fig. 2. At first the 398-nm excitation beam was incident on the specimens. A small polaron is formed by the photon absorption, and the STE formation mediated by the intrinsic surface states and defects is accompanied by the photon emission. In the bulk $SrTiO_3$, it is impossible to observe the STE luminescence at temperatures above 110 K due to its weak binding energy and short radiative lifetime.

FT infrared spectroscopy was measured to examine organic substance in the specimens. Figure 3 shows a weak C−H absorption peak near 2880 cm^{-1} caused by the residual organic substance. With increasing annealing temperature the peak decreases. The C−H absorption peak has completely vanished when the temperature reaches above 650 °C. In the low-frequency region there are two bands at 1520 and 1340 cm^{-1} attributed to asymmetric and symmetric vibrations of the C=O groups, respectively. It is clearly seen that the bands decrease with increasing annealing temperature and

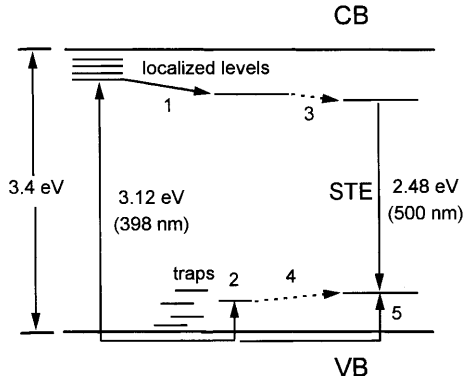

Fig. 2. Schematic diagram of the PL process in the nanophase $SrTiO_3$. (1) Small-polaron formation. (2) possible hole capture. (3) and (4) retarded formation of a STE. (3) and (5) direct formation of a STE

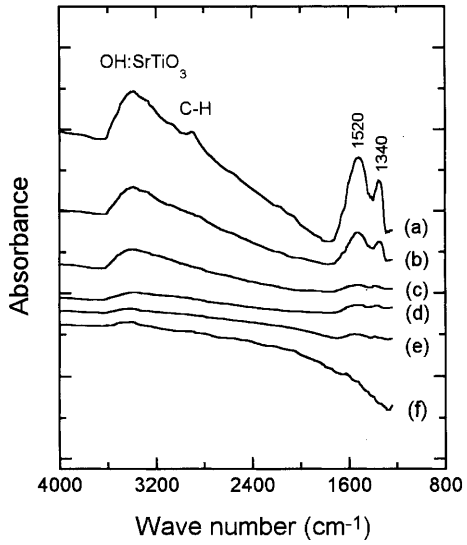

Fig. 3. FT infrared spectra of the nanophase $SrTiO_3$ annealed for 3 hours at various temperatures: (a) 450 °C, (b) 550 °C, (c) 650 °C, (d) 750 °C, (e) 850 °C and (f) 900 °C

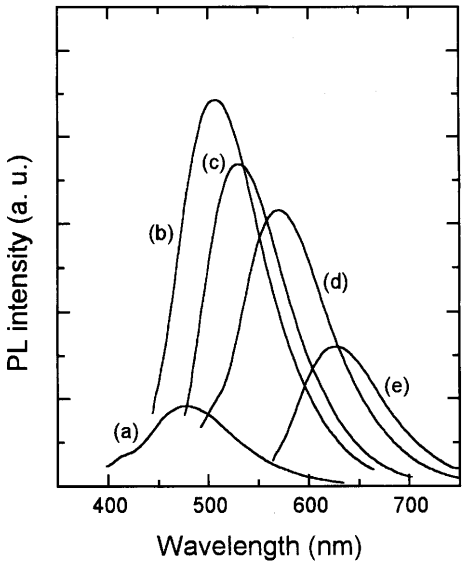

Fig. 4. PL spectra of the nanophase $SrTiO_3$ (26 nm) under excitation with different wavelengths: (a) 370 nm, (b) 430 nm, (c) 480 nm, (d) 520 nm, and (e) 600 nm

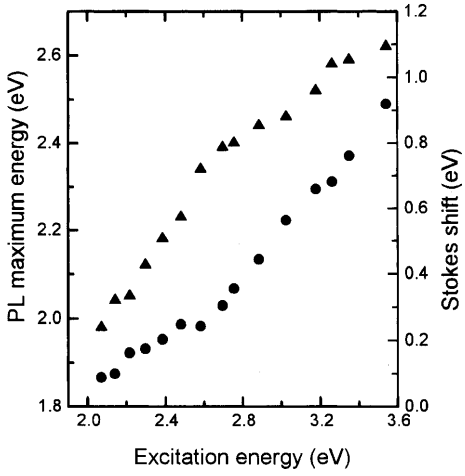

Fig. 5. PL maximum energy (*triangle*) and Stokes shifts (*dot*) as a function of excitation energy

tend to enter the background near 650 °C. The FT infrared spectrum clearly indicates that the residual organic substance does not make a contribution to luminescence in the annealing temperature region from 650 to 900 °C.

Figure 4 exhibits the PL spectra of the nanophase $SrTiO_3$ with the size of 26 nm under different excitation wavelengths. A set of emission bands are distinctly recorded under various wavelengths, and the peak position of each band shifts upward with increasing excitation wavelength. This means that a series of the STE levels are formed in the forbidden gap. It should be pointed out that the visible emission band could not be observed under excitation with the wavelength longer than 600 nm shown in triangle notation in Fig. 5, which means that there is a lowest position of the localized levels in the forbidden gap, corresponding to the energy of the excitation wavelength of 600 nm. In a sense, the strength of the electron–phonon interaction can be signified by the difference between the excitation energy and the emission maximum (Stokes shift). It can be seen from the dot notation in Fig. 5 that the Stokes shift decreases with decreasing the excitation energy. This indicates a dependence of electron–phonon interaction on the excitation energy, related to the formation of a series of the STE levels. These experimental data imply that the optical response region of the nanophase $SrTiO_3$ can be continuously extended from the ultraviolet to the visible region, which is of great significance in optoelectronic applications, such as in photocatalysis and photoelectric conversion for effectively use of solar energy.

The PL spectra of the nanophase $SrTiO_3$ (26 nm) under different excitation wavelengths were also recorded at liquid-nitrogen temperature. A part of these PL spectra is plotted in Fig. 6 where a blueshift is shown with regard to the corresponding peak in Fig. 4. In addition, it was found that all the low-temperature visible emission bands become more intensive and more narrow compared to those at room temperature. Moreover, for the excitation with wavelength longer than 480 nm, the visible emission band was almost vanishing.

There are two competitive processes associated with the STE: one is the STE recombination resulting in the visible

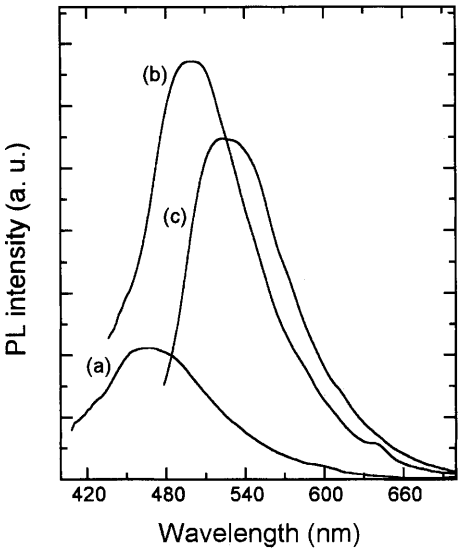

Fig. 6. PL spectra of the nanophase $SrTiO_3$ (26 nm) under excitation with different wavelengths: (a) 370 nm, (b) 430 nm, and (c) 480 nm at liquid-nitrogen temperature

emission and the other is the thermal dissociation of the STE making the emission quench. Since the thermal dissociation process dramatically drops at lower temperature, the emission via the recombination of STE was relatively intensified. The broadening of the emission band is mainly caused by the Doppler and thermal-collision mechanisms. The lowering of temperature reduces the broadening effect indeed, therefore the linewidth of the emission band was observed to decrease at liquid-nitrogen temperature. Also, the lowering of temperature would result in the shallower localized levels and the weaker electron–phonon interaction, and the STE level would shift to a higher position, leading to the blueshift of the emission band.

3 Conclusion

The observed visible emission bands in the nanophase $SrTiO_3$ show that the properties of the electronic states are strongly related to particle size and temperature. The visible emission band is ascribed to the recombination of the long-lived STE with the forceful binding energy which can be established in the nanostructured $SrTiO_3$ at room temperature. The excitation-wavelength dependence of the visible emission band indicates that there are a series of STE levels related to the intrinsic surface states and defect centers in the nanophase $SrTiO_3$. Such kinds of the nanophase $SrTiO_3$ are a promising candidate for wide applications in the field of photocatalysis, photochromics, and photoelectric conversion due to its broad optic-response range from the ultraviolet to visible light.

Acknowledgements. This work has been supported by the National Climbing Project of Fundamental Research of China. The authors would like to thank Dr. Zuliang Du for his technical assistance and valuable discussion.

References

1. M.L. Steiqerwald, J. Am. Chem. Soc. **110**, 3046 (1988)
2. Y. Wang, N. Herron: J. Phys. Chem. **92**, 4988 (1988)
3. T. Takagahara, K. Takeda: Phys. Rev. B **46**, 15578 (1992)
4. K.A. Müller: Phys. Rev. Lett. **2**, 314 (1959)
5. K.A. Müller, H. Burkard: Phys. Rev. B **19**, 3593 (1979)
6. D.E. Grupp, A.M. Goldman: Science **276**, 392 (1997)
7. A.H. Kahn, A.J. Leyendecker: Phys. Rev. A **135**, 1321 (1964)
8. M. Capizzi, A. Frova: Phys. Rev. Lett. **25**, 1298 (1970)
9. K.W. Blazey: Phys. Rev. Lett. **27**, 146 (1971)
10. H. Ihrig, J.H.T. Hengst, M. Klerk: Z. Phys. B **40**, 301 (1981)
11. L. Grabner: Phys. Rev. **177**, 1315 (1969)
12. Y.T. Sihvonen: J. Appl. Phys. **38**, 4431 (1967)
13. H. Ihrig, M. Klerk: Appl. Phys. Lett. **35**, 307 (1979)
14. M. Aguilar, F. Agullo-Lopez: J. Appl. Phys. **53**, 9009 (1982)
15. R. Leonelli, J.L. Brebner: Solid State Commun. **54**, 505 (1985)
16. R. Leonelli, J.L. Brebner: Phys. Rev. B **33**, 8649 (1986)
17. E.M. Shahverdiev: Physica B **192**, 274 (1993)
18. E.M. Shahverdiev, M. Ilhan: Physica B **193**, 177 (1994)
19. H. Vogt: Phys. Rev. B **51**, 8046 (1995)
20. J.F. Meng, Y.B. Huang, W.F. Zhang, Z.L. Du, Z.Q. Zhu, G.T. Zou: Phys. Lett. A **205**, 72 (1995)
21. C. Liu, J. Zhong, Y. Li, Z. Zhang: Acta Phys. Sin., **47**, 1680 (1998)
22. W.F. Zhang, X.T. Zhang, Z. Yin, M.S. Zhang, G.H. Ma, Z.L. Du, Chin: Phys. Lett. **15**, 758 (1998)
23. K. Ishikawa, K. Yoshikawa, N. Ukada: Phys. Rev. B **37**, 5852 (1988)
24. J.H. Yang, Y.J. Hong, Y.B. Bai, Y.Y. Wang, X.T. Zhang, D.J. Wang, T.J. Li: Acta Scientiarum Naturalium Universitatis Jilinensis, **1**, 71 (1997)
25. L. Zhou, S.Y. Zhang, S.W. Fu, Z. Wang, L.D. Zhang: Acta Phys. Sin. **146**, 994 (1997)
26. L. Zhou, X.J. Liu, S.Y. Zhang, J.C. Wang, L.D. Zhang: Mater. Sci. Eng. B **49**, 117 (1997)
27. R. Courths, J. Noffke, H. Wern, R. Heise: Phys. Rev. B **42**, 9127 (1990)
28. S. Ellialtioglu, T. Wolfram: Phys. Rev. B **18**, 4509 (1978)
29. T. Wolfram, F.J. Morin, R. Hurst: In NBS special publication, No. 455, Electrocatalysis on Non-metallic Surfaces, ed. by A.D. Franklin (US Government Printing Office, Washington, DC 1975) p. 21
30. B. Zou, L. Xiao, T. Li, J. Zhao, Z. Lai, S. Gu: Appl. Phys. Lett. **59**, 1826 (1991)
31. B. Zou, Y. Zhang, L. Xiao, T. Li: J. Appl. Phys. **73**, 4689 (1993)